frontiers | Frontiers in Materials

TYPE Original Research
PUBLISHED 21 November 2025
DOI 10.3389/fmats.2025.1668454

Check for updates

OPEN ACCESS

EDITED BY
Qiang Chen,
Southeast University, China

REVIEWED BY
Mahboubeh Nabavinia,
The Research Institute at Nationwide Children's Hospital, United States
Ziwen Wang,
University of Wisconsin-Madison, United States

*CORRESPONDENCE
Xieping Dong,
13576030901@163.com

RECEIVED 18 July 2025
REVISED 28 September 2025
ACCEPTED 20 October 2025
PUBLISHED 21 November 2025

CITATION
Su S, Yang K, Zeng Y and Dong X (2025) A multifunctional cryogel for enhanced angiogenesis and osteogenesis in bone tissue engineering.
Front. Mater. 12:1668454.
doi: 10.3389/fmats.2025.1668454

COPYRIGHT
© 2025 Su, Yang, Zeng and Dong. This is an open-access article distributed under the terms of the Creative Commons Attribution License (CC BY). The use, distribution or reproduction in other forums is permitted, provided the original author(s) and the copyright owner(s) are credited and that the original publication in this journal is cited, in accordance with accepted academic practice. No use, distribution or reproduction is permitted which does not comply with these terms.

A multifunctional cryogel for enhanced angiogenesis and osteogenesis in bone tissue engineering

Shenghui Su[1,2], Ke Yang[2], Yu Zeng[1,3] and Xieping Dong[1]*

[1]JXHC Key Laboratory of Digital Orthopaedics, Jiangxi Provincial People's Hospital, The First Affiliated Hospital of Nanchang Medical College, Nanchang, Jiangxi, China, [2]Institute of Metal Research, Chinese Academy of Science, Shenyang, Liaoning, China, [3]Jiangxi University of Chinese Medicine, Nanchang, Jiangxi, China

Bone defects exceeding self-repair capacity remain a major clinical challenge, necessitating biomaterial-based strategies for effective regeneration. This study developed a multifunctional cryogel integrating copper-containing mesoporous bioactive glass (Cu-MBG) and bone marrow mesenchymal stem cell-derived exosomes (BMSC-Exos) into a decellularized extracellular matrix (dECM). The cryogel's physicochemical properties, including structure, morphology, porosity, degradation, and mechanical strength, were characterized, confirming its suitability for bone tissue engineering. *In vitro* studies demonstrated that Cu-MBG/Exos@dECM enhanced osteogenic differentiation and promoted angiogenesis by releasing bioactive copper ions from Cu-MBG and regulating cell proliferation and differentiation via BMSC-Exos. Additionally, the cryogel provided a biomimetic microenvironment supporting cell adhesion and extracellular matrix remodeling, synergistically promoting bone regeneration. These findings highlight Cu-MBG/Exos@dECM as a promising biomaterial for bone repair, offering an effective and advanced strategy for treating bone defects.

KEYWORDS

mesoporous bioactive glass, decellularized extracellular matrix, copper ions, exosomes, angiogenesis, osteogenesis

1 Introduction

The management of skeletal defects, particularly those exceeding critical dimensions caused by trauma, disease, or developmental disorders, remains a formidable challenge in contemporary orthopedics (Hench and Thompson, 2010; Aldhaher et al., 2023). Although autologous bone transplantation represents the current therapeutic standard, its clinical implementation faces substantial constraints due to harvest site complications and finite tissue sources (Li W. et al., 2023). Alternative approaches utilizing

allografts or xenografts introduce concerns regarding immune responses and pathogen transfer risks (Abodunrin et al., 2023).

These challenges inherent in traditional transplantation techniques have driven advances in tissue engineering strategies, particularly in scaffold development (O'Keefe and Mao, 2011; Koushik et al., 2023). Decellularized extracellular matrix (dECM) scaffolds stand out among emerging biomaterials because they provide a unique environment that retains the complex spatial structure and bioactive elements of native tissues while removing potentially immunogenic cellular components (Hinderer et al., 2016). These nature-inspired structures exhibit superior biological functions and provide a better environment for cell activation than traditional synthetic matrices (Hoshiba, 2019; Dhandayuthapani et al., 2011). Advances in bone regeneration strategies have led to increasing interest in mesoporous bioactive glass (MBG), a material known for its tissue compatibility and osteoinductive properties (Eriksson et al., 2021; He et al., 2023). The addition of copper ions (Cu^{2+}) to the MBG structure marks a key innovation in scaffold engineering (Salvo and Sandoval, 2022). These ions exhibit bifunctional properties, stimulating angiogenesis through *HIF-1α* signaling and promoting osteocyte development through various cellular pathways (Li Y. et al., 2023).

Cell-free regenerative approaches have advanced significantly with the discovery that bone marrow mesenchymal stem cells (BMSCs) release therapeutic nanovesicles (Heldring et al., 2015). These exosome (Exo) carries specific molecular signals that enhance tissue healing processes without triggering immune responses (Bagno et al., 2018). Their ability to simultaneously support bone formation and vascularization makes them particularly valuable for skeletal tissue engineering (Lou et al., 2017).

Our study has developed an advanced multifunctional bone implant scaffold that combined Copper-containing mesoporous bioactive glass (Cu-MBG) with BMSC-derived exosomes in dECM. This innovative design could combine the excellent performance of dECM, the dual-action properties of copper ions, and the tissue repair function mediated by exosomes to produce a synergistic effect. This new material (Cu-MBG/EXOs@dECM) provides new possibilities for solving the current limitations of bone defect treatment and provides a good theoretical basis for the development of regenerative medicine.

In addition to addressing critical-sized bone defects, this study reflects a broader trend in regenerative medicine involving the development of multifunctional and cell-free platforms with strong translational potential. The incorporation of Cu-MBG and exosomes into a biologically derived scaffold not only enhances regenerative outcomes but also aligns with the ongoing transition away from cell-based therapies, which are often limited by regulatory concerns, storage issues, and immunological risks (Qin et al., 2022). Furthermore, this composite system enables precise regulation of osteogenic and angiogenic processes, offering a valuable *in vitro* model for exploring the mechanisms of bone healing and tissue remodeling. By integrating materials science, cell biology, and clinical needs, this work contributes to the advancement of next-generation smart biomaterials capable of meeting the complex requirements of bone tissue engineering.

2 Materials and methods

2.1 Reagents and materials

Chemical components were sourced from reputable suppliers:Tetraethyl Orthosili-cate (TEOS),$CuCl_2{\cdot}H_2O$,$Ca(NO_3)_2{\cdot}4H_2O$ and Triethyl Phosphate (TEP) (Sigma-Aldrich); cell culture essentials including PBS,Dulbecco's Modified Eagle Medium (DMEM), and Fetal Bovine Serum (FBS) (Gibco); Cetyltrimethylammonium Bromide (CTAB),eth-anol,and ammonium hydroxide (Aladdin Chemistry). All substances were analytical grade and utilized as received. The porcine skin in this study were purchased from Beijing Ruijian High-Tech Biotechnology Co., Ltd (Beijing, China). The cell lines of BMSCs (CRL-12424) in this study were obtained from the American Type Culture Collection (Manassas, United States). The cell lines of HUVECs (HUVEC-20001) in this study were obtained from Cyagen Biosciences (Guangdong, China). The studies involving animals were reviewed and approved by the Medical Ethics Committee of Jiangxi Provincial People's Hospital (2021-051).

2.2 Cu-MBG nanoparticle synthesis and characterization

Cu-MBG nanoparticles were fabricated using a modified sol-gel technique. CTAB was dissolved in deionized water. Ethyl acetate was added after complete dissolution. The above solution was stirred at 300 rpm and NH_4OH (2 mL) was added after 30 min. TEOS, TEP, and $Ca(NO_3)_2{\cdot}4H_2O$ were added in turn every half an hour, followed by $CuCl_2{\cdot}2H_2O$. The mixture was stirred at room temperature for 24 h,then centrifuged, washed, and heat treated at 650 °C for 6 h.

Scanning electron microscopy (SEM) (Merlin, Carl Zeiss AG, Germany), transmission electron microscopy (TEM) (JEM-2100HR, Japan), Energy-dispersive X-ray spectroscopy (EDS) (ThermoFisher Scientific, Waltham, MA, United States) and X-ray diffraction spectrometer (XRD) (X'pert PRO, PANalytical, Netherlands) were used to analyze the physical and chemical properties of Cu-MBG,including morphology, internal structure and elemental composition.

The degradation behavior of Cu-MBG nanoparticles was evaluated under simulated physiological conditions. Briefly, 10 mg Cu-MBG was immersed in 10 mL PBS and incubated at 37 °C under constant shaking. At predetermined time points, the samples were collected, centrifuged, washed, and dried to a constant weight. The remaining weight was measured and expressed as a percentage of the initial dry weight.

2.3 BMSCs exosome extraction and characterization

BMSCs were cultured in exosome-free medium. Cell debris was removed by centrifugation at 300 g (10 min) and 2000 g (20 min), followed by ultracentrifugation at 100,000 g (70 min). The pellet was washed with PBS and ultracentrifuged again. Exosomes were characterized by TEM and other methods.

Transmission electron microscopy (TEM) analysis of exosomes was performed using a field emission transmission electron microscope (HT7700, Hitachi, Japan). The mass concentration of exosomes was adjusted to 0.5 g/L, and after resuspending in PBS, 2.5% glutaraldehyde was added for fixation for 10 min 20-30 μL of the fixed exosome suspension was dropped on the carbon film-coated copper grid, and allowed to stand at room temperature for 1 min, dried under infrared light for 5 min, and a drop of 5% phosphoric acid solution was added to the copper grid for staining at room temperature for 5-10 min, the phosphoric acid solution was absorbed, and dried under infrared light for 10 min. Finally, the sample was observed under TEM at a magnification of 50000 times.

The particle size distribution was measured using a Zetasizer Nano ZSE (Malvern Instruments, UK). The mass concentration of the exosomes was adjusted to 1 g/L, and each measurement was repeated three times. The particle size data was obtained by dynamic light scattering and analyzed using the Zetasizer software. Data of at about 1000 particles were collected for each sample to ensure statistical reliability.

2.4 dECM production

Porcine skin underwent decellularization using a specialized solution (50 mM Tris-HCl, 5 mM EDTA, 1% Triton X-100, 0.1% SDS, pH 7.4) for 48 h, followed by DNase I treatment (100 U/mL, 24 h). After thorough PBS rinsing, the dECM was freeze-dried, ground, and stored at −80 °C.

2.5 Composite cryogel engineering

Lyophilized dECM was dissolved at 4 °C to obtain a clear, ice-cold solution. Cu-MBG nanoparticles were first pre-wetted in a small volume of the dECM solution and added dropwise under continuous gentle magnetic stirring (300–400 rpm, on ice) for 10–15 min until no visible aggregates were observed. Subsequently, exosomes were introduced as the last component into the nanoparticle–dECM mixture and gently stirred (200–300 rpm, on ice) for 5–10 min to avoid foaming and shear-induced vesicle damage. The resulting homogeneous precursor was immediately cast into molds. This mixture was cross-linked with 0.5% glutaraldehyde (−10 °C,4 days),subjected to three freeze-thaw cycles, and extensively washed to remove excess crosslinker.

2.6 Cryogel physical and chemical properties characterization

An fourier transform infrared (FTIR) spectrometer (Thermo Fisher) was used to analyze the chemical composition of the Cryogel. SEM imaging was performed on gold-coated samples. Mechanical characteristics were assessed with a universal testing machine (Instron 5967) at 1 mm/min compression, recording stress-strain data. Cryogel samples were submerged in PBS (pH 7.4, 37 °C) under gentle motion,at specific time points (1, 2, 3, 5, 7,9 days), specimens were extracted, lyophilized, and weighed to calculate mass loss. Porosity was evaluated using drainage method.

2.7 Cell seeding

The BMSCs used in this study were all isolated from mice and all the experiments were performed using cells at passage 4. Aspirate the old mBMSCs culture medium and rinse three times with PBS buffer. Add 1 mL of trypsin and incubate in a 37 °C incubator for 1 min. Terminate the digestion process by adding 3 mL of complete culture medium. Centrifuge at 1000 rpm for 5 min and discard the supernatant. Add the culture medium to the cells and pipette evenly to obtain a uniform cell suspension. Count the cells using a cell counter and seed the cells at a concentration of 5×10^4 cells/mL in a 24-well plate. The seeding method of HUVECs is consistent with that of mBMSCs,but the cell concentration is 1×10^5.

2.8 Cellular viability assessment

mBMSCs were cultured in culture medium at 37 °C, 5% CO_2. Cell viability was assessed using CCK-8 assay and live/dead staining (calcein-AM, propidium iodide) at 1, 3, and 5 days after seeding.

After 24 h of cell culture, samples were rinsed with PBS and fixed with 4% paraformaldehyde for 30 min. After permeabilization with 0.1% Triton X-100 for 10 min, cells were stained with phalloidin for 1 h and DAPI for 5 min in the dark. Fluorescence images were captured using a confocal microscope.

2.9 Osteogenic differentiation analysis

Aspirate the old mBMSCs culture medium and rinse three times with PBS buffer. Add 1 mL of trypsin and incubate in a 37 °C incubator for 1 min. Terminate the digestion process by adding 3 mL of complete culture medium. Centrifuge at 1000 rpm for 5 min and discard the supernatant. Add the culture medium to the cells and pipette evenly to obtain a uniform cell suspension. Count the cells using a cell counter and seed the cells at a concentration of 5×10^4 cells/mL in a 24-well plate.

mBMSCs were cultured under osteogenic conditions (standard medium plus 10 mM β-glycerophosphate, 50 μg/mL ascorbic acid, 100 nM dexamethasone) for 7 days, Alkaline phosphatase (ALP) activity and expression of osteogenic markers (*ALP*, *RUNX2*, *OCN*, *OPN*) were evaluated using established protocols. After 14 days of culture, the degree of mineralization was assessed using Alizarin red staining (ARS).

2.10 Angiogenesis evaluation

CD31 immunofluorescence staining was performed on Human umbilical vein endothelial cells (HUVECs) seeded in confocal dishes, followed by fixation, permeabilization, blocking, primary and secondary antibody incubation, and nuclear staining. The fluorescence signals were then observed using confocal microscopy and analyzed with ImageJ.

The vasculogenic mimicry of HUVECs was evaluated using a Matrigel tube formation assay. In brief, 60 μL of Matrigel (Corning, United States) was added to a 96-well plate and polymerized at 37 °C for 1 h. After cell passage, activity detection

and counting, HUVECs were seeded onto the Matrigel-coated wells and incubated at 37 °C. Following incubation, tube-like structures were visualized under a microscope (Olympus, Japan), and their formation was quantified using ImageJ software. The expression of angiogenic markers (*VEGF*, *HIF-1α*) were assessed using established protocols.

2.11 Data analysis

Results were presented as mean ± SD from triplicate experiments. Statistical analysis employed one-way ANOVA (GraphPad Prism 10.1.2). Significance was set at $p < 0.05$.

3 Results

3.1 Synthesis and characterization of Cu-MBG and exos

In this study, Cu-MBG and Exos were synthesized and characterized. TEM images showed that the Cu-MBGs were clearly distinguishable, highly ordered in arrangement, and uniform in pore size (Figure 1A). SEM images revealed that the Cu-MBG powder consisted of densely packed nanospheres (Figure 1B). EDS results confirmed the successful incorporation of copper into the mesoporous bioactive glass powder (Figure 1C). XRD analysis showed that the Cu-MBG did not exhibit obvious crystalline diffraction peaks (Figure 1D).

TEM images showed that the exosomes were roughly spherical in shape (Figure 1E). The particle size distribution of the exosomes, measured using a Malvern Nano Laser Particle Analyzer, ranged from 100 to 300 nm,which was consistent with the typical size range for exosomes (Figure 1F).

The degradation curve of Cu-MBG nanoparticles (Figure 1G) showed the weight degradation was fast at an early stage, but the degradation process was slow and controllable after 50 h, and the residual weight was still more than 80% of the initial mass after 120 h. This degradation trend indicates that Cu-MBG nanoparticles have good long-term stability, which is conducive to the sustained release of ions and the extension of bioactivity in the composite scaffold.

3.2 Synthesis and characterization of Cu-MBG/EXOs@dECM

In the FTIR spectrum, the absorption peaks for Cu-MBG at 475 cm^{-1}, 800 cm^{-1}, and 1100 cm^{-1} correspond to the asymmetric stretching vibration of Si-O-Si,the symmetric stretching vibration of Si-O, and the symmetric bending vibration of Si-O-Si, respectively. For the group containing dECM, absorption peaks at 1700-1600 cm^{-1} and 1600-1500 cm^{-1} correspond to the amide I and amide II bands of proteins. The composite bioactive glass and dECM group retained the characteristic absorption peaks of both components (Figure 2A). As shown in Figure 2B, all three cryogel groups exhibited a microporous structure with good pore morphology and uniform pore wall thickness. In the Cu-MBG/dECM and Cu-MBG/EXOs@dECM groups, evenly distributed mesoporous bioactive glass particles were observed. The compression modulus and swelling rate of Cu-MBG/dECM and Cu-MBG/EXOs@dECM groups were not significantly different,but were significantly different compared with the dECM group (Figures 2C,D). Degradation curve analysis revealed that the weight loss at various time points in the Cu-MBG/dECM and Cu-MBG/EXOs@dECM groups was not significantly different, and both exhibited slower degradation compared to the dECM group (Figure 2E). There was no significant difference in the porosity of the three groups of materials (Figure 2F).

3.3 *In vitro* biocompatibility

Strong biocompatibility is crucial for biomaterials. The survival and proliferation of cells were evaluated by seeding BMSCs on the surface of the cryogel. Live/dead staining performed after co-culturing for 1, 3, and 5 days showed that almost all cells exhibited green fluorescence (Figure 3A). The optical density values of the four groups gradually increased at 1, 3, and 5 days, indicating that the cells continued to proliferate, and there was no significant difference among the four groups (Figure 3B).

As shown in Figures 3C,D, fluorescence staining showed significant differences in cell morphology between different groups. The cells in the control group aggregated and exhibited poor spreading. In contrast, the cells of the Cu-MBG/dECM and Cu-MBG@EXOs/dECM groups had enhanced spreading and extended pseudopodia.

3.4 Osteogenic differentiation of BMSCs on Cu-MBG/EXOs@dECM

The osteogenic effect of the cryogels was evaluated by culturing BMSCs on the surface of the cryogels. mRNA expression analysis was analyzed after 7 days of osteogenic induction, and the mRNA expression levels of *ALP*, *OPN*, *RUNX2*, and *OCN* further confirmed this result (Figures 4A–D). After 7 and 14 days of osteogenic induction, ALP and ARS staining were observed on all cryogel surfaces,and the staining of Cu-MBG/EXOs@dECM cryogels was stronger compared with the Cu-MBG/dECM and dECM groups (Figures 4E,G). The results of quantitative analysis were consistent with the qualitative observations (Figures 4F,H).

3.5 *In vitro* angiogenesis assay of Cu-MBG/EXOs@dECM

HUVECs were used to model endothelial progenitor cells *in vitro* and investigate the direct effect of Cu-MBG/EXOs@dECM on their angiogenic potential. As expected, the presence of Cu-MBG/EXOs@dECM promoted more sprouting of blood vessel buds compared to the other two groups, which was reflected in the results of the tube formation assay (Figure 5A). Quantitative analysis showed significant differences in the total length, number

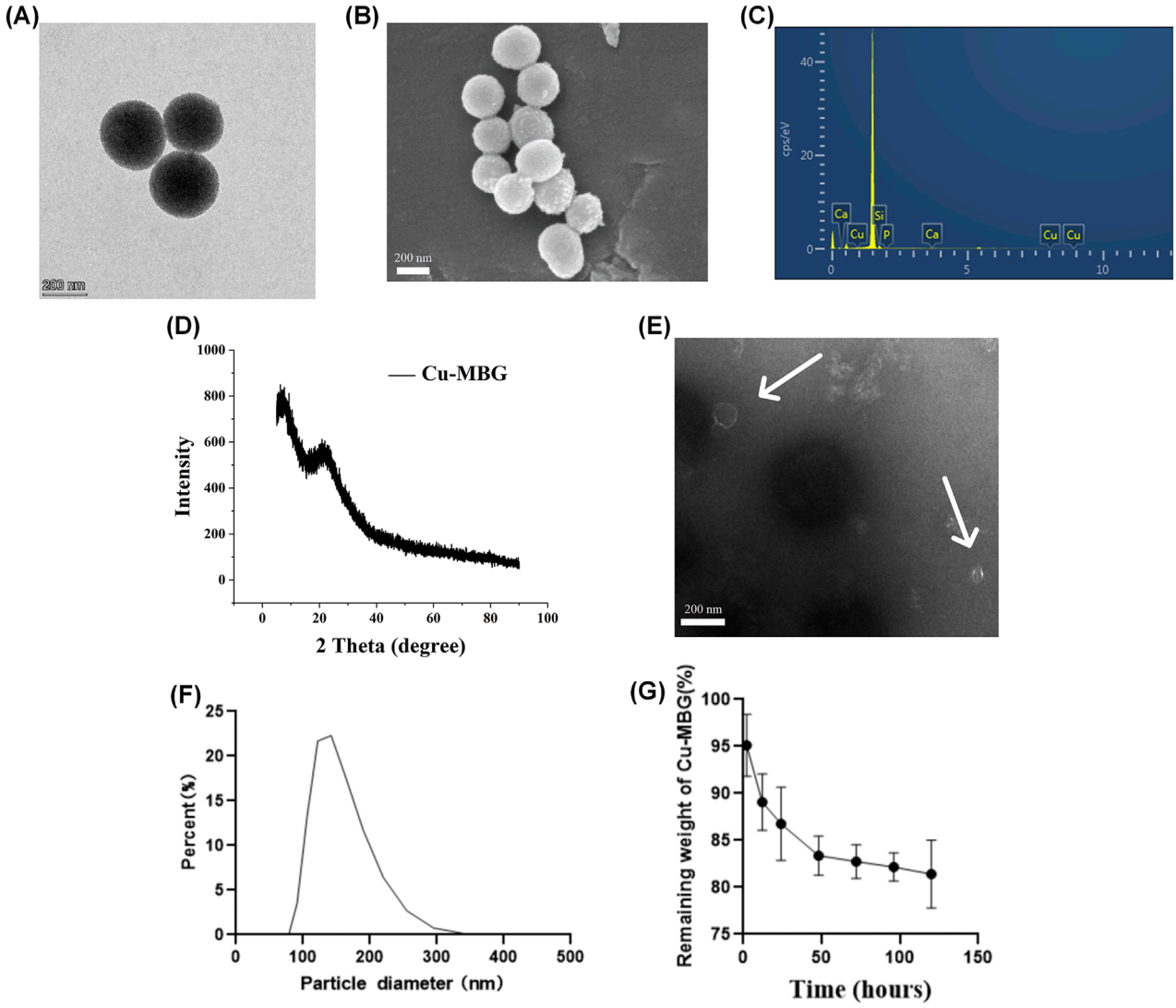

FIGURE 1
Characterization of Cu-MBG nanoparticles and exosomes. **(A)** TEM image of Cu-MBG showing its mesoporous structure. **(B)** SEM image of Cu-MBG nanoparticles. **(C)** EDS of Cu-MBG confirming elemental composition. **(D)** XRD pattern of Cu-MBG. **(E)** TEM image of exosomes displaying their spherical morphology. **(F)** Size distribution of exosomes. **(G)** Degradation curve of Cu-MBG nanoparticles (n = 3). (*p < 0.05,**p < 0.01,***p < 0.001, and ****p < 0.0001).

of junctions,and number of meshes of the vascular networks among the different groups (Figures 5B–D).

To evaluate the angiogenic potential of the materials in promoting angiogenesis,CD31 immunofluorescence staining was performed. The immunofluorescence staining results showed that in the control group, CD31-positive staining of HUVECs was sparse, and the fluorescence intensity was weak, indicating low angiogenic activity of endothelial cells without any biomaterial intervention. In comparison to the control group and Cu-MBG/dECM group,the Cu-MBG/EXOs@dECM group exhibited the most significant CD31-positive staining, with the highest fluorescence intensity and the greatest number of CD31-positive cells (Figure 5E). Additionally, qRT-PCR results showed that angiogenic genes in the Cu-MBG/EXOs@dECM group, including *VEGF* and *HIF-1α*, were significantly upregulated (Figures 5F,G).

4 Discussion

Bone is a dynamic tissue with inherent repair and regeneration capabilities, allowing it to self-heal following injury (Bernhard et al., 2017). However, in the case of large defects, spontaneous repair is often insufficient and biomaterials need to be implanted to promote osteogenesis (Barreto et al., 2022). Recent progress in bone tissue engineering has emphasized the need for multifunctional scaffolds that not only support bone regeneration but also modulate the microenvironment to enhance osteogenesis and angiogenesis. For instance, a study by Zhang et al. reported the incorporation of magnesium ascorbyl phosphate (MAP) into GelMA hydrogels for cranial defect repair, demonstrating that MAP not only enhanced mineralization of BMSCs but also activated ERK/AKT signaling to promote vascularization and bone healing

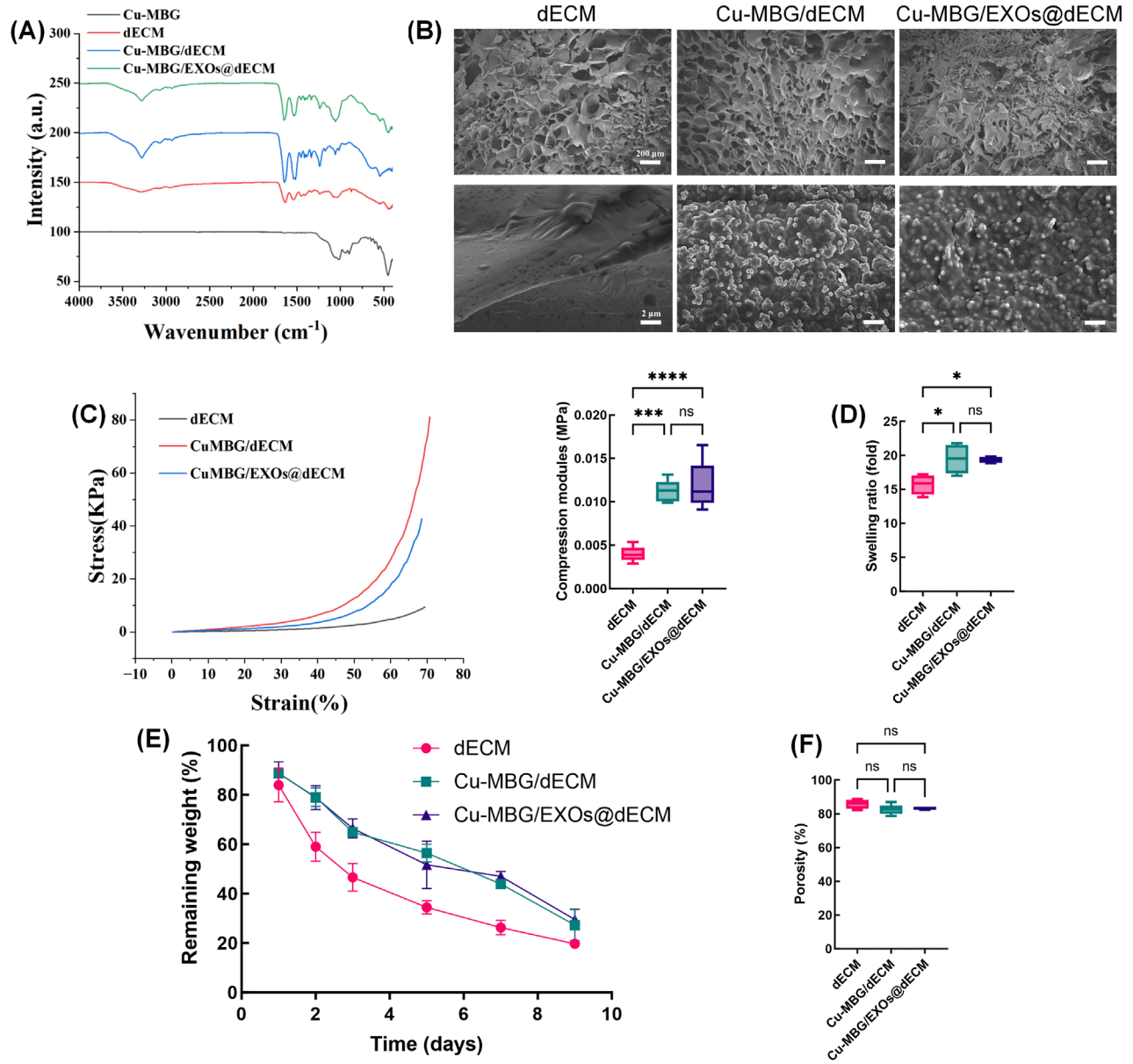

FIGURE 2
Structural and physicochemical characterization of Cu-MBG/EXOs@dECM. **(A)** FTIR spectra of Cu-MBG/EXOs@dECM. **(B)** SEM images of Cu-MBG/EXOs@dECM. **(C)** Compression modulus of Cu-MBG/EXOs@dECM (n = 3). **(D)** Swelling rate of Cu-MBG/EXOs@dECM (n = 3). **(E)** Degradation profile of Cu-MBG/EXOs@dECM (n = 3). **(F)** Porosity analysis of Cu-MBG/EXOs@dECM (n = 3). (*p < 0.05,**p < 0.01,***p < 0.001, and ****p < 0.0001).

without exogenous calcium supplementation (Zhang et al., 2023). In another investigation, Huang et al. developed a food-derived tofu/GelMA hybrid hydrogel with favorable mechanical properties and immunomodulatory effects, which significantly improved bone regeneration during *in vivo* implantation (Huang et al., 2020). Moreover, a review published in iScience summarized the potential of non-coding RNA (ncRNA)-based therapies and delivery scaffolds in promoting osteogenic differentiation and bone defect repair, highlighting the emerging role of gene-regulating materials in this field (Guan et al., 2022). These studies underscore the growing consensus that scaffolds designed for bone repair should integrate biological functionality, bioactivity modulation, and molecular-level regulation, which aligns well with our current strategy of incorporating Cu-MBG and exosomes within a dECM-based cryogel scaffold.

In recent years, dECM has gained attention as a promising alternative for bone regeneration scaffolds due to its ability to provide a biomimetic environment that supports tissue development. Firstly, dECM scaffolds preserve macrostructural characteristics, including overall geometry and a highly porous architecture, along with microstructural features such as surface roughness and microporosity,all of which contribute significantly to enhanced osteoinductivity (He et al., 2020). Secondly,the rigid matrix mimics the crosslinked collagen

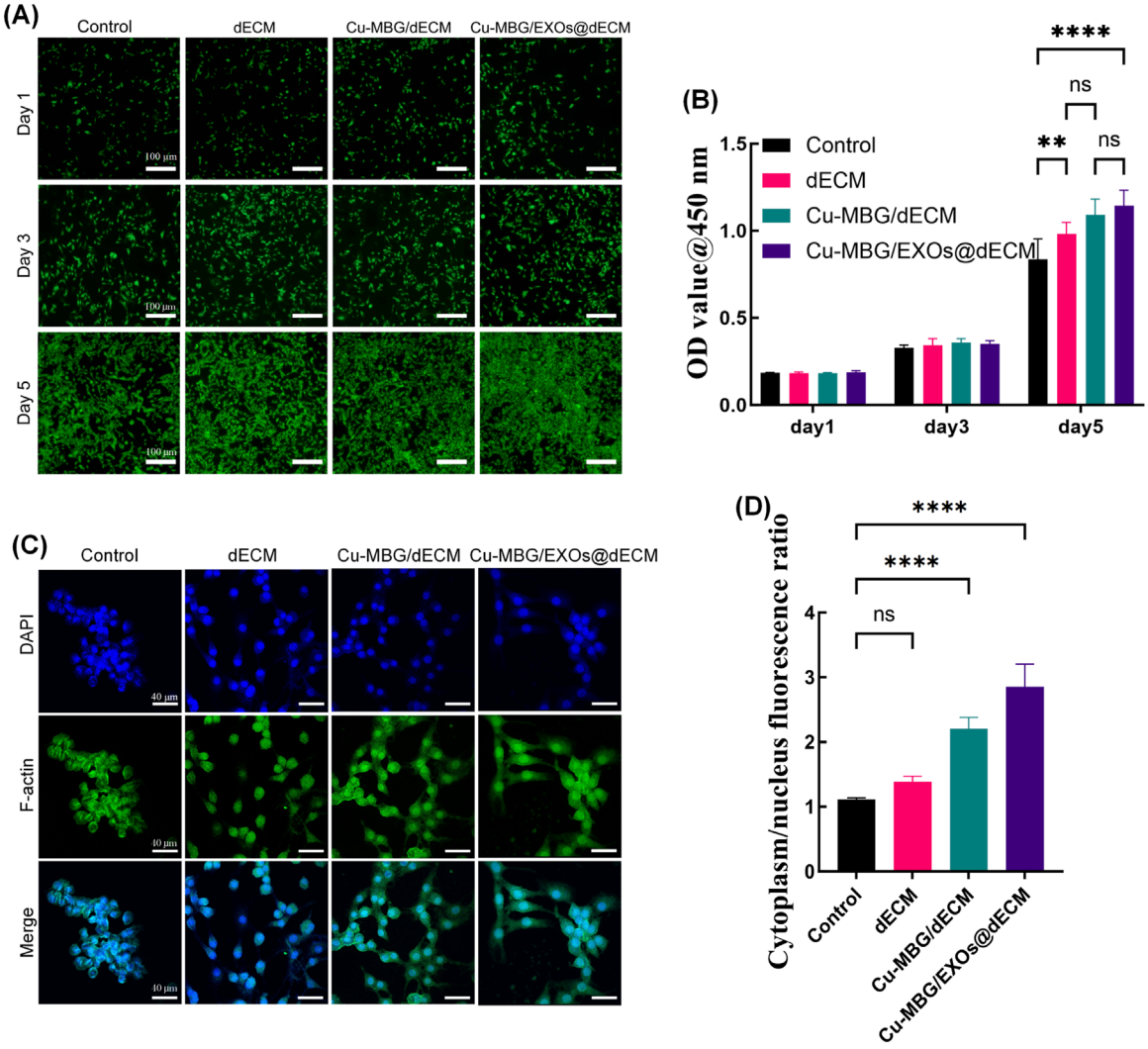

FIGURE 3
In vitro biocompatibility assessment of Cu-MBG/EXOs@dECM. **(A)** Live/dead staining of BMSCs cultured on different groups at 1, 3, and 5 days. **(B)** CCK-8 assay results showing cell proliferation on different groups over time (n = 3). **(C,D)** Cell morphology assay and quantitative analysis of BMSCs after 24 h of culture (n = 3). (*p < 0.05, **p < 0.01, ***p < 0.001, and ****p < 0.0001).

framework found in native bone, which directs stem cells toward osteogenic differentiation upon implantation (Engler et al., 2006). Thirdly, dECM scaffolds preserve immunomodulatory cytokines, including transforming growth factor-β (TGF-β), bone morphogenetic proteins (BMPs), and basic fibroblast growth factor (bFGF), which regulate inflammatory responses (Xie et al., 2020).

In this study, Cu-MBG was successfully prepared by combining the template method with the sol-gel method. This method is a simple and effective method for synthesizing nanomaterials. Its advantage is that it can achieve precise control over the morphology, structure and function of the material. This method has broad application prospects in the preparation of mesoporous materials, especially in the biomedical field (Zarkov, 2024). The synergistic relationship between angiogenesis and bone development has been widely studied (Kanczler and Oreffo, 2008; Tao et al., 2022). Copper added to mesoporous bioactive glass has angiogenic properties, which can significantly enhance its osteogenic potential. The vascular network has dual functions, promoting metabolic support and actively regulating bone regeneration through complex cell signaling mechanisms (Huang et al., 2022). Our study showed that copper also directly promoted osteogenic differentiation through various pathways, including enhancing the expression of bone-specific genes and increasing matrix mineralization. Specifically, copper-rich materials showed increased expression of bone formation markers (such as *ALP*, *RUNX2*, *OCN* and *OPN*), as well as increased ALP and ARS activity levels. At the molecular level, Cu^{2+} regulates MSC differentiation and bone remodeling through the Wnt signaling cascade (Liu et al., 2022). Components of this pathway, especially c-Myc and Akt, can also enhance *HIF-1α* expression and promote vascular development (Tan et al., 2021).

Previous studies have demonstrated that copper-containing biomaterials can promote both angiogenesis and osteogenesis,

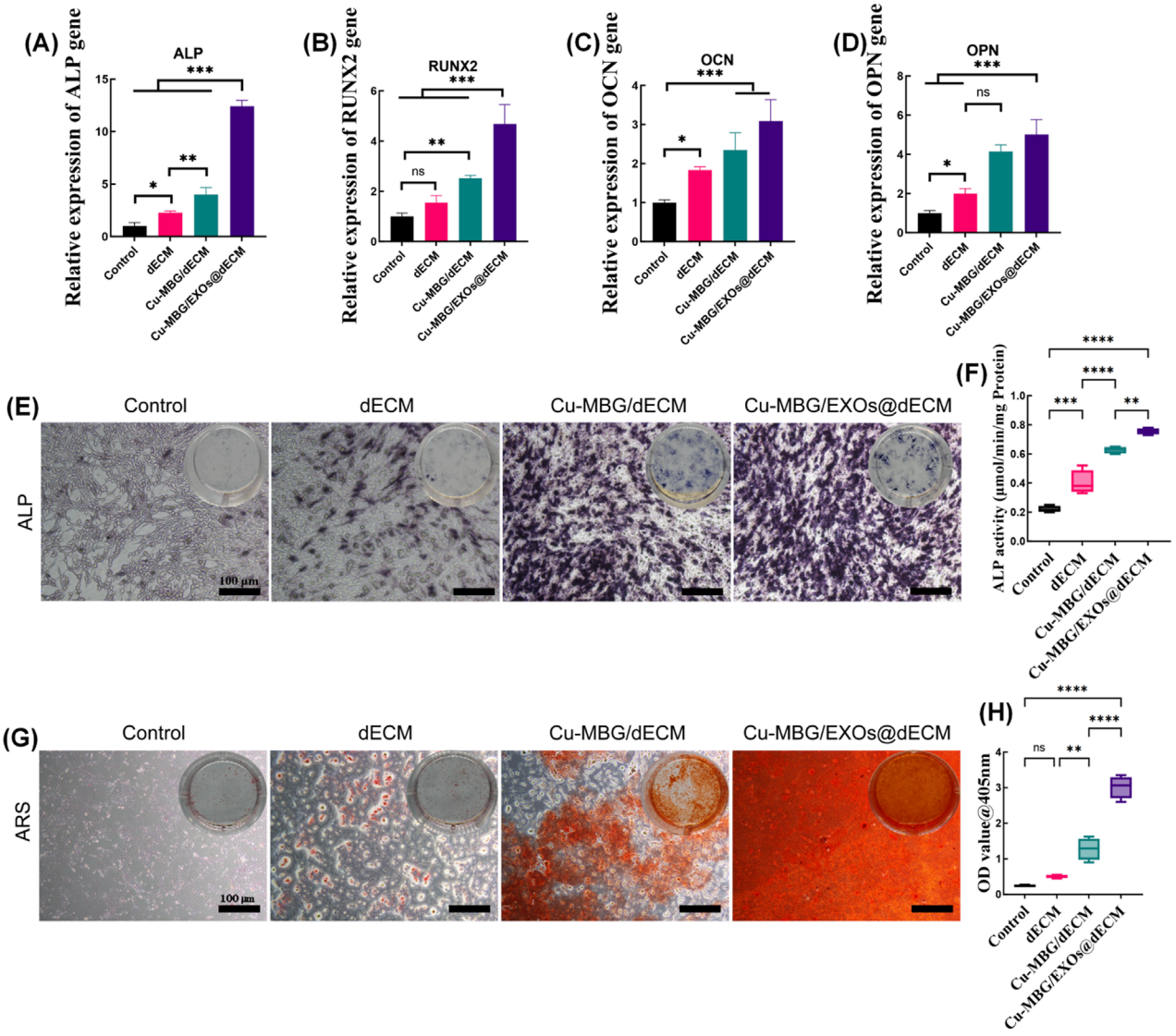

FIGURE 4
Osteogenic differentiation of BMSCs on Cu-MBG/EXOs@dECM. **(A–D)** qRT-PCR analysis showing upregulated expression of osteogenic markers (*ALP*, *OPN*, *RUNX2*, and *OCN*) after 7 days of cultivation (n = 3). **(E,F)** ALP staining and quantitative analysis of BMSCs cultured on different Cryogel after 7 days (n = 3). **(G,H)** ARS staining and quantitative analysis of BMSCs cultured on different Cryogel after 14 days (n = 3). (*p < 0.05, **p < 0.01, ***p < 0.001, and ****p < 0.0001).

primarily through the release of Cu^{2+}. For example, a recent study using Ti6Al4V-4.5Cu alloys fabricated by selective laser melting found that the released copper ions enhanced the expression of proangiogenic genes in preosteoblasts, which in turn stimulated vascular formation in endothelial cells, thereby supporting the coupling of osteogenesis and angiogenesis (Li Y. et al., 2023). Another review emphasized that copper nanoparticles actively participate in all phases of wound healing, particularly by promoting angiogenesis via *HIF-1α* activation and *VEGF* expression, highlighting the key regulatory role of copper in tissue regeneration (Salvo and Sandoval, 2022). Our study confirmed that the inclusion of Cu-MBG in the cryogel significantly upregulated osteogenic gene expression and enhanced vascular network formation *in vitro*. Compared to these systems, our Cu-MBG-based cryogel integrates copper within a mesoporous network, allowing for sustained ion release and spatial control, thereby enhancing both osteogenic gene expression and extracellular matrix remodeling. This suggests that our composite scaffold not only matches but may surpass previously reported Cu-MBG systems in promoting bone regeneration through synergistic interactions with exosomes and the dECM scaffold.

MSC-derived exosomes represent key mediators in tissue repair, functioning as biological carriers for various regulatory molecules (Heldring et al., 2015). These vesicles encompass numerous proteins and microRNAs (Chen et al., 2010), orchestrating tissue regeneration through multiple pathways which include stem cell activation, cell survival promotion, immune response modulation, vascular formation,and so on (Hassanzadeh et al.,

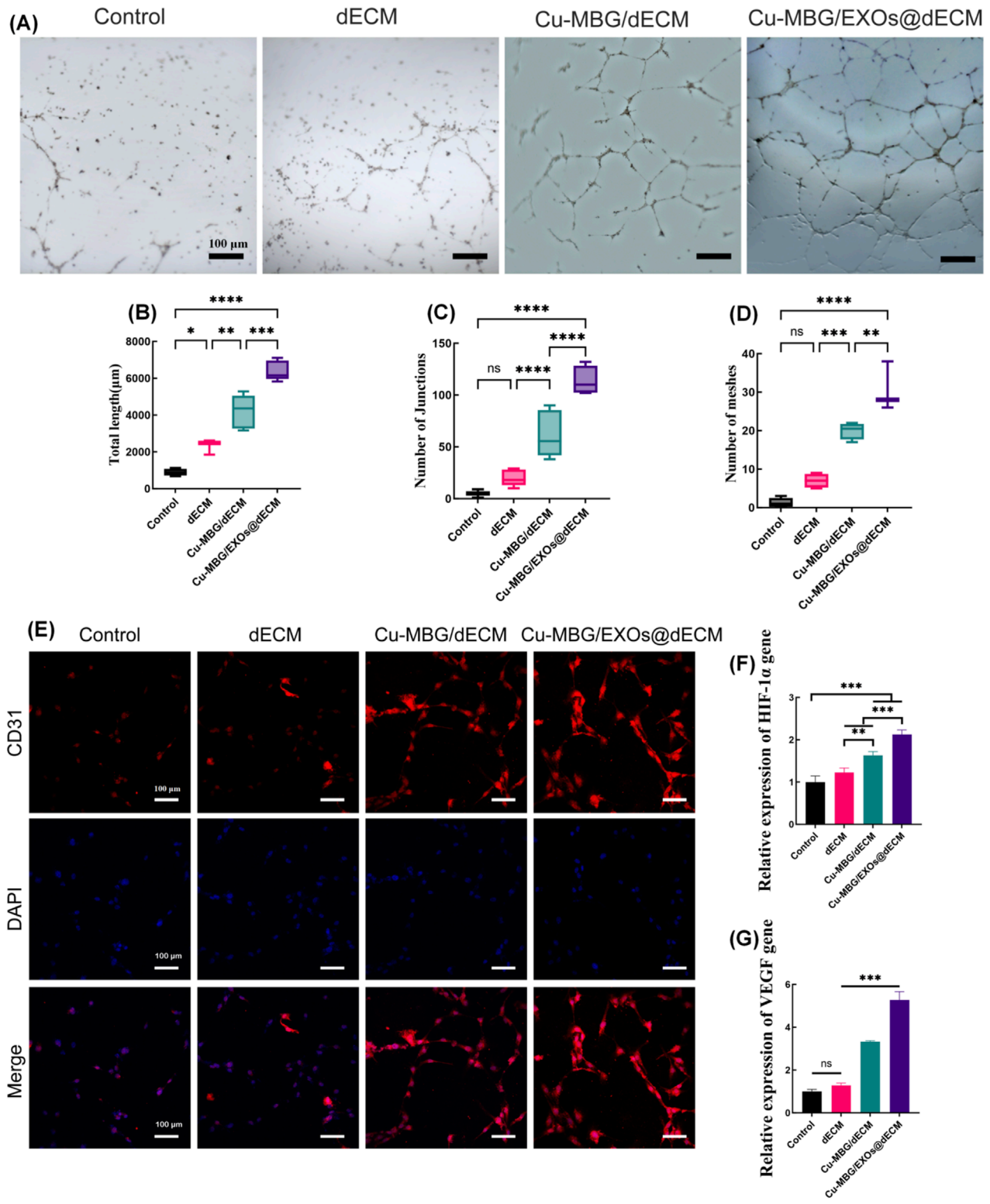

FIGURE 5
In vitro angiogenesis assay of Cu-MBG/EXOs@dECM. **(A)** Tube formation assay of HUVECs cultured on different groups. **(B–D)** Quantitative analysis of total tube length, number of junctions, and mesh formation (n = 3). **(E)** CD31 immunofluorescence staining of HUVECs cultured on different Cryogel. **(F,G)** qRT-PCR analysis of angiogenic markers *VEGF* and *HIF-1α*(n = 3). (*p < 0.05,**p < 0.01,***p < 0.001, and ****p < 0.0001).

2021). Previous studies have shown that BMSC-derived exosomes may exhibit special effects in bone formation, regulating macrophage behavior and enhancing angiogenesis through activation of the BMP-2/Smad1/RUNX2 pathway (Bagno et al., 2018). Recent studies have demonstrated that fluorine-engineered exosomes can significantly enhance cellular uptake and angiogenic activity, offering a promising strategy to improve the therapeutic efficacy of exosome-based regenerative therapies (Ma et al., 2023). Our study verified the important role of BMSC-exosomes in angiogenesis and bone formation in experimental models.

The novel combination of Cu-MBG, BMSC-exosomes, and dECM creates an advanced platform for bone regeneration. The integrated system exhibits a strong synergistic effect, with dECM providing an optimized environment for controlled delivery of therapeutic components while maintaining key biological signals,and Cu-MBG and exosomes producing a strong synergistic effect in promoting osteogenesis and angiogenesis. This approach overcomes the limitations of traditional single components,and this integrated strategy provides new opportunities for customized bone tissue engineering applications. Future developments may combine other better bioactive components or engineered exosomes to further enhance the regenerative effect.

This multifunctional cryogel platform holds promise for clinical translation in the treatment of large or complex bone defects, particularly in scenarios where traditional grafts or cell-based therapies are limited by donor site morbidity, immune rejection, or regulatory constraints. The combination of a biologically derived scaffold, bioactive ions, and naturally secreted exosomes offers a cell-free strategy that is inherently safer, easier to store and transport, and more compliant with current good manufacturing practices. Given its demonstrated ability to promote both angiogenesis and osteogenesis, this composite material has the potential to be a therapeutic option for bone repair in orthopedic, maxillofacial, and dental surgical settings. The results of this study underscore the substantial potential of these multifunctional cryogels as advanced scaffolds for bone regeneration. Beyond their demonstrated capacity to support both osteogenesis and angiogenesis, the modular nature of these scaffolds offers significant flexibility for clinical translation. They can potentially be combined with patient-derived cells, growth factors, or approved pharmacological agents to tailor regenerative strategies for individual patients, enabling personalized therapy. With appropriate preclinical validation and manufacturing optimization, this approach has the potential to advance toward clinical trials and ultimately contribute to improved patient outcomes in regenerative medicine.

5 Conclusion

Our study demonstrated that the innovative Cu-MBG/EXOs@dECM composite system effectively integrated the structural framework of dECM, the dual osteogenic and angiogenic properties of copper,and the regenerative potential of exosomes. This composite material exhibited excellent effects in promoting the simultaneous occurrence of angiogenesis and osteogenesis, significantly improving bone repair in severe defect models. This new tissue engineering protocol provides a promising solution for challenging bone reconstruction cases.

Data availability statement

The original contributions presented in the study are included in the article/supplementary material, further inquiries can be directed to the corresponding author.

Ethics statement

The animal study was approved by the Medical Ethics Committee of Jiangxi Provincial People's 92 Hospital (2021-051). The study was conducted in accordance with the local legislation and institutional requirements.

Author contributions

SS: Writing – original draft, Writing – review and editing. KY: Writing – review and editing. YZ: Writing – review and editing. XD: Writing – review and editing.

Funding

The author(s) declare that financial support was received for the research and/or publication of this article. This work was supported by National Natural Science Foundation of China (grant number 82460425) and Jiangxi Provincial Health Technology Project (grant number 202510141).

Conflict of interest

The authors declare that the research was conducted in the absence of any commercial or financial relationships that could be construed as a potential conflict of interest.

Generative AI statement

The author(s) declare that no Generative AI was used in the creation of this manuscript.

Any alternative text (alt text) provided alongside figures in this article has been generated by Frontiers with the support of artificial intelligence and reasonable efforts have been made to ensure accuracy, including review by the authors wherever possible. If you identify any issues, please contact us.

Publisher's note

All claims expressed in this article are solely those of the authors and do not necessarily represent those of their affiliated organizations, or those of the publisher, the editors and the reviewers. Any product that may be evaluated in this article, or claim that may be made by its manufacturer, is not guaranteed or endorsed by the publisher.

References

Abodunrin, O. D., El Mabrouk, K., and Bricha, M. (2023). A review on borate bioactive glasses (BBG): effect of doping elements, degradation, and applications. *J. Mater. Chem. B* 11 (5), 955–973. doi:10.1039/d2tb02505a

Aldhaher, A., Shahabipour, F., Shaito, A., Al-Assaf, S., Elnour, A. A. M., Sallam, E. B., et al. (2023). 3D hydrogel/bioactive glass scaffolds in bone tissue engineering: status and future opportunities. *Heliyon* 9 (7), e17050. doi:10.1016/j.heliyon.2023.e17050

Bagno, L., Hatzistergos, K. E., Balkan, W., and Hare, J. M. (2018). Mesenchymal stem cell-based therapy for cardiovascular disease: progress and challenges. *Mol. Ther. J. Am. Soc. Gene Ther.* 26 (7), 1610–1623. doi:10.1016/j.ymthe.2018.05.009

Barreto, M. E. V., Medeiros, R. P., Shearer, A., Fook, M. V. L., Montazerian, M., and Mauro, J. C. (2022). Gelatin and bioactive glass composites for tissue engineering: a review. *J. Funct. Biomater.* 14 (1), 23. doi:10.3390/jfb14010023

Bernhard, J., Ferguson, J., Rieder, B., Heimel, P., Nau, T., Tangl, S., et al. (2017). Tissue-engineered hypertrophic chondrocyte grafts enhanced long bone repair. *Biomaterials* 139, 202–212. doi:10.1016/j.biomaterials.2017.05.045

Chen, T. S., Lai, R. C., Lee, M. M., Choo, A. B., Lee, C. N., and Lim, S. K. (2010). Mesenchymal stem cell secretes microparticles enriched in pre-microRNAs. *Nucleic acids Res.* 38 (1), 215–224. doi:10.1093/nar/gkp857

Dhandayuthapani, B., Yoshida, Y., Maekawa, T., and Kumar, D. S. (2011). Polymeric scaffolds in tissue engineering application: a review. *Int. J. Polym. Sci.* 2011 (1), 1–19. doi:10.1155/2011/290602

Engler, A. J., Sen, S., Sweeney, H. L., and Discher, D. E. (2006). Matrix elasticity directs stem cell lineage specification. *Cell* 126 (4), 677–689. doi:10.1016/j.cell.2006.06.044

Eriksson, E., Björkenheim, R., Strömberg, G., Ainola, M., Uppstu, P., Aalto-Setälä, L., et al. (2021). S53P4 bioactive glass scaffolds induce BMP expression and integrative bone formation in a critical-sized diaphysis defect treated with a single-staged induced membrane technique. *Acta biomater.* 126, 463–476. doi:10.1016/j.actbio.2021.03.035

Guan, S., Zhang, Z., and Wu, J. (2022). Non-coding RNA delivery for bone tissue engineering: progress, challenges, and potential solutions. *iScience* 25 (8), 104807. doi:10.1016/j.isci.2022.104807

Hassanzadeh, A., Rahman, H. S., Markov, A., Endjun, J. J., Zekiy, A. O., Chartrand, M. S., et al. (2021). Mesenchymal stem/stromal cell-derived exosomes in regenerative medicine and cancer; overview of development, challenges, and opportunities. *Stem cell Res. and Ther.* 12 (1), 297. doi:10.1186/s13287-021-02378-7

He, J., Li, Z., Yu, T., Wang, W., Tao, M., Ma, Y., et al. (2020). Preparation and evaluation of acellular sheep periostea for guided bone regeneration. *J. Biomed. Mater. Res. Part A* 108 (1), 19–29. doi:10.1002/jbm.a.36787

He, L., Yin, J., and Gao, X. (2023). Additive manufacturing of bioactive glass and its polymer composites as bone tissue engineering scaffolds: a review. *Bioeng. Basel, Switz.* 10 (6), 672. doi:10.3390/bioengineering10060672

Heldring, N., Mäger, I., Wood, M. J., Le Blanc, K., and Andaloussi, S. E. (2015). Therapeutic potential of multipotent mesenchymal stromal cells and their extracellular vesicles. *Hum. gene Ther.* 26 (8), 506–517. doi:10.1089/hum.2015.072

Hench, L. L., and Thompson, I. (2010). Twenty-first century challenges for biomaterials. *J. R. Soc. Interface* 7 (Suppl. 4), S379–S391. doi:10.1098/rsif.2010.0151.focus

Hinderer, S., Layland, S. L., and Schenke-Layland, K. (2016). ECM and ECM-Like materials - biomaterials for applications in regenerative medicine and cancer therapy. *Adv. drug Deliv. Rev.* 97, 260–269. doi:10.1016/j.addr.2015.11.019

Hoshiba, T. (2019). Decellularized extracellular matrix for cancer research. *Mater. Basel, Switz.* 12 (8), 1311. doi:10.3390/ma12081311

Huang, K., Gu, Z., and Wu, J. (2020). Tofu-Incorporated hydrogels for potential bone regeneration. *ACS biomaterials Sci. and Eng.* 6 (5), 3037–3045. doi:10.1021/acsbiomaterials.9b01997

Huang, J., Han, Q., Cai, M., Zhu, J., Li, L., Yu, L., et al. (2022). Effect of angiogenesis in bone tissue engineering. *Ann. Biomed. Eng.* 50 (8), 898–913. doi:10.1007/s10439-022-02970-9

Kanczler, J. M., and Oreffo, R. O. (2008). Osteogenesis and angiogenesis: the potential for engineering bone. *Eur. cells and Mater.* 15, 100–114. doi:10.22203/ecm.v015a08

Koushik, T. M., Miller, C. M., and Antunes, E. (2023). Bone tissue engineering scaffolds: function of multi-material hierarchically structured scaffolds. *Adv. Healthc. Mater.* 12 (9), e2202766. doi:10.1002/adhm.202202766

Li, W., Wu, Y., Zhang, X., Wu, T., Huang, K., Wang, B., et al. (2023a). Self-healing hydrogels for bone defect repair. *RSC Adv.* 13 (25), 16773–16788. doi:10.1039/d3ra01700a

Li, Y., Luo, W., Liu, Y., Lu, Y., Geng, W., and Lin, J. (2023b). Copper-containing titanium alloys promote the coupling of osteogenesis and angiogenesis by releasing copper ions. *Biochem. biophysical Res. Commun.* 681, 157–164. doi:10.1016/j.bbrc.2023.09.072

Liu, J., Xiao, Q., Xiao, J., Niu, C., Li, Y., Zhang, X., et al. (2022). Wnt/β-catenin signalling: function, biological mechanisms, and therapeutic opportunities. *Signal Transduct. Target. Ther.* 7 (1), 3. doi:10.1038/s41392-021-00762-6

Lou, G., Chen, Z., Zheng, M., and Liu, Y. (2017). Mesenchymal stem cell-derived exosomes as a new therapeutic strategy for liver diseases. *Exp. and Mol. Med.* 49 (6), e346. doi:10.1038/emm.2017.63

Ma, S., Song, L., Bai, Y., Wang, S., Wang, J., Zhang, H., et al. (2023). Improved intracellular delivery of exosomes by surface modification with fluorinated peptide dendrimers for promoting angiogenesis and migration of HUVECs. *RSC Adv.* 13 (17), 11269–11277. doi:10.1039/d3ra00300k

O'Keefe, R. J., and Mao, J. (2011). Bone tissue engineering and regeneration: from discovery to the clinic–an overview. *Tissue Eng. Part B, Rev.* 17 (6), 389–392. doi:10.1089/ten.teb.2011.0475

Qin, J., Li, M., Yuan, M., Shi, X., Song, J., He, Y., et al. (2022). Gallium(III)-Mediated dual-cross-linked alginate hydrogels with antibacterial properties for promoting infected wound healing. *ACS Appl. Mater. and interfaces* 14 (19), 22426–22442. doi:10.1021/acsami.2c02497

Salvo, J., and Sandoval, C. (2022). Role of copper nanoparticles in wound healing for chronic wounds: literature review. *Burns and trauma* 10, tkab047. doi:10.1093/burnst/tkab047

Tan, Z., Zhou, B., Zheng, J., Huang, Y., Zeng, H., Xue, L., et al. (2021). Lithium and copper induce the osteogenesis-angiogenesis coupling of bone marrow mesenchymal stem cells *via* crosstalk between canonical wnt and HIF-1α signaling pathways. *Stem Cells Int.* 2021, 1–15. doi:10.1155/2021/6662164

Tao, J., Miao, R., Liu, G., Qiu, X., Yang, B., Tan, X., et al. (2022). "Spatiotemporal correlation between HIF-1α and bone regeneration,"*FASEB J.* 36 10, e22520. doi:10.1096/fj.202200329rr

Xie, X., Wang, W., Cheng, J., Liang, H., Lin, Z., Zhang, T., et al. (2020). Bilayer pifithrin-α loaded extracellular matrix/PLGA scaffolds for enhanced vascularized bone formation. *Colloids surfaces B, Biointerfaces* 190, 110903. doi:10.1016/j.colsurfb.2020.110903

Zarkov, A. (2024). Sol-Gel technology applied to materials science: synthesis, characterization and applications. *Mater. Basel, Switz.* 17 (2), 462. doi:10.3390/ma17020462

Zhang, Z., Hao, Z., Xian, C., Zhang, J., and Wu, J. (2023). Triple functional magnesium ascorbyl phosphate encapsulated hydrogel: a cosmetic ingredient promotes bone repair *via* anti-oxidation, calcium uptake and blood vessel remodeling. *Chem. Eng. J.* 472, 145061. doi:10.1016/j.cej.2023.145061